PHYSICAL REVIEW D **73,** 014024 (2006)

Branching ratio and polarization of $B \to \rho(\omega)\rho(\omega)$ decays in perturbative QCD approach

Ying Li* and Cai-Dian Lü

CCAST (World Laboratory), P.O. Box 8730, Beijing 100080, China
Institute of High Energy Physics, P.O. Box 918(4), Beijing 100049, China†

(Received 20 September 2005; published 25 January 2006)

In this work, we calculate the branching ratios, polarization fractions and *CP* asymmetry parameters of decay modes $B \to \rho(\omega)\rho(\omega)$ in the perturbative QCD approach, which is based on $\mathbf{k}_T$ factorization. After calculation, we find that the branching ratios of $B^0 \to \rho^+\rho^-$, $B^+ \to \rho^+\rho^0$, and $B^+ \to \rho^+\omega$ are at the order of 10^{-5}, and their longitudinal polarization fractions are more than 90%. The above results agree with BaBar's measurements. We also calculate the branching ratios and polarization fractions of $B^0 \to \rho^0\rho^0$, $B^0 \to \rho^0\omega$, and $B^0 \to \omega\omega$ decays. We find that their longitudinal polarization fractions are suppressed to 60–80% due to a small color suppressed tree contribution. The dominant penguin and nonfactorization tree contributions equally contribute to the longitudinal and transverse polarization, which will be tested in the future experiments. We predict the *CP* asymmetry of $B^0 \to \rho^+\rho^-$ and $B^+ \to \rho^+\rho^0$, which will be measured in *B* factories.

DOI: 10.1103/PhysRevD.73.014024 PACS numbers: 13.25.Hw

I. INTRODUCTION

The study of exclusive nonleptonic weak decays of *B* mesons provides not only good opportunities for testing the standard model (SM) but also powerful means for probing different new physics scenarios beyond the SM. The mechanism of two body *B* decay is still not quite clear, although many physicists are devoted to this field. The hadronic effects must be important while a reliable calculation of these effects is very difficult [1]. Starting from the factorization hypothesis [2], many approaches have been built to explain the existing data and made some progress such as generalized factorization [3], QCD factorization (BBNS) [4], perturbative QCD approach (PQCD) [5], and soft-collinear effective theory (SCET) [6]. These approaches separately explained many of the $B \to PP$ and $B \to PV$ decays though some flaws existed in different approaches.

Recently, $B \to VV$ decays such as $B \to \phi K^*$ [7], $B \to \rho K^*$ [8], have aroused many interests of physicists. It is known that both longitudinal and transverse polarization states are possible in $B \to VV$ decay modes. So, the theoretical analysis of $B \to VV$ is more complicated than $B \to PP$ and $B \to PV$. The predictions of those decays' polarization fractions according to the naive factorization do not agree with the experimental results, although many ideas [9–11] have been proposed to explain this phenomenon. Some people think that it is a signal of new physics [12,13]. Very recently, both BaBar and Belle have measured the branching ratios and polarizations of the decays $B^0 \to \rho^+\rho^-$ and $B^+ \to \rho^+\rho^0$ [14–17], some decay modes have very large branching ratios. The longitudinal polarization fractions are also very large, which are different from that of $B \to \phi K^*$.

*Electronic address: liying@mail.ihep.ac.cn
†Mailing address.

In this paper, we will study the branching ratios, polarization fractions and *CP* violation parameters of $B \to \rho(\omega)\rho(\omega)$ decays in the PQCD approach. At the rest frame of *B* meson, the *B* meson decays to light vector mesons with large momentum. Because the two light mesons move fast back to back, they have small chance to exchange soft particles, therefore the soft final state interaction may not be important. A hard gluon emitted from the four quark operator kicks the light slow spectator quark in *B* meson with large momentum transfer to form a fast moving final state meson. Therefore, the short distance hard process dominates this decay amplitude. In this factorization theorem, decay amplitude is written as the convolution of the corresponding hard parts with universal meson distribution amplitudes, which describe nonperturbative hadronic process of the decay. Because the Sudakov effect from k_T and threshold resummation [18], the end point singularities do not appear.

This paper is organized as follows. In Sec. II, we give some ingredients of the basic formalism. The numerical results for branching ratios and *CP* asymmetry are given in Sec. III and IV respectively. We summarize our work in Sec. V.

II. FORMALISM

The recently developed PQCD approach is based on the k_T factorization scheme, where three energy scales are involved [5]. The hard dynamics are characterized by $\sqrt{m_B\Lambda_{\rm QCD}}$, which is to be perturbatively calculated in PQCD. The harder dynamics is from m_W scale to m_B scale described by renormalization group equation for the four quark operators. The dynamics below $\sqrt{m_B\Lambda_{\rm QCD}}$ is soft, which is described by the meson wave functions. The soft dynamics is not perturbative but universal for all channels. Based on this factorization, the $B \to \rho\rho$ decay amplitude is written as the following factorizing formula [19],

$$\mathcal{M} \sim \int dx_1 dx_2 dx_3 b_1 db_1 b_2 db_2 b_3 db_3 \times \mathrm{Tr}[C(t)\Phi_B(x_1, b_1) \times \Phi_\rho(x_2, b_2)\Phi_\rho(x_3, b_3)H(x_i, b_i, t)S_t(x_i)e^{-S(t)}], \quad (1)$$

where Tr denotes the trace over Dirac and color indices. $C(t)$ is Wilson coefficient of the four quark operator which results from the radiative corrections at short distance. The wave function Φ_M absorbs nonperturbative dynamics of the process, which is process independent. The hard part H is rather process dependent and can be calculated in perturbative approach. t is chosen as the largest energy scale in the hard part, to kill the largest logarithm. The jet function $S_t(x_i)$, called threshold resummation, comes from the resummation of the double logarithms $\ln^2 x_i$. The Sudakov form factor $S(t)$ is from the resummation of double logarithms $\ln^2 Qb$ [5,19].

A. Wave function

In this paper, we use the light-cone coordinates to describe the four dimension momentum as $(p^+, p^-, p^\perp)$. The B meson is treated as a heavy-light system, whose wave function is defined as

$$\Phi^{(\mathrm{in})}_{B,\alpha\beta,ij} \equiv \langle 0|\bar{b}_{\beta j}(0)d_{\alpha i}(z)|B(p)\rangle = \frac{i\delta_{ij}}{\sqrt{2N_c}}\int dx d^2\mathbf{k}_T e^{-i(xp^-z^+ - \mathbf{k}_T\mathbf{z}_T)} \times [(\not{p} + M_B)\gamma_5 \phi_B(x, \mathbf{k}_T)]_{\alpha\beta}, \quad (2)$$

where the indices α and β are spin indices, i and j are color indices, and $N_c = 3$ is the color factor. The distribution amplitude ϕ_B is normalized as

$$\int_0^1 dx_1 \phi_B(x_1, b_1 = 0) = \frac{f_B}{2\sqrt{2N_c}}, \quad (3)$$

where b_1 is the conjugate space coordinate of transverse momentum k_T, and f_B is the decay constant of the B meson. In this study, we use the model function

$$\phi_B(x, b) = N_B x^2(1-x)^2 \exp\left[-\frac{1}{2}\left(\frac{xM_B}{\omega_B}\right)^2 - \frac{\omega_B^2 b^2}{2}\right], \quad (4)$$

where N_B is the normalization constant. We use $\omega_B = 0.4$ GeV, which is determined by the calculation of form factors and other well known decay modes [5].

As a light-light system, The ρ^- meson wave function of the longitudinal part is given by [20]

$$\Phi_{\rho^-,\alpha\beta,ij} \equiv \langle \rho(p, \epsilon_L)|\bar{d}_{\beta j}(z)u_{\alpha i}(0)|0\rangle = \frac{\delta_{ij}}{\sqrt{2N_c}}\int_0^1 dx e^{ixp\cdot z}[m_\rho \not{\epsilon}_L \phi_\rho(x) + \not{\epsilon}_L \not{p}\phi^t_\rho(x) + m_\rho \phi^s_\rho(x)]_{\alpha\beta}. \quad (5)$$

The first term in the above equation is the leading twist wave function (twist-2), while the others are subleading twist (twist-3) wave functions. The ρ meson can also be transversely polarized, and its wave function is then

$$\langle \rho^-(p, \epsilon_T)|\bar{d}_{\beta j}(z)u_{\alpha i}(0)|0\rangle = \frac{\delta_{ij}}{\sqrt{2N_c}}\int_0^1 dx e^{ixp\cdot z} \times \left\{\not{\epsilon}_T[\not{p}\phi^T_\rho(x) + m_\rho \phi^v_\rho(x)] + \frac{m_\rho}{p\cdot n} i\epsilon_{T\mu\nu\rho\sigma}\gamma_5\gamma^\mu \times \epsilon^\nu p^\rho n^\sigma \phi^a_\rho(x)\right\}, \quad (6)$$

where n is the moving direction of ρ particle. Here the leading twist wave function for the transversely polarized ρ meson is the first term which is proportional to ϕ^T_ρ.

The distribution amplitudes of ρ meson, ϕ_ρ, ϕ^t_ρ, ϕ^s_ρ, ϕ^T_ρ, ϕ^v_ρ, and ϕ^a_ρ, are calculated using light-cone QCD sum rule [20]:

$$\phi_\rho(x) = \frac{3f_\rho}{\sqrt{2N_c}}x(1-x)[1 + 0.18C_2^{3/2}(2x-1)], \quad (7)$$

$$\phi^t_\rho(x) = \frac{f^T_\rho}{2\sqrt{2N_c}}\{3(2x-1)^2 + 0.3(2x-1)^2[5(2x-1)^2 - 3] + 0.21[3 - 30(2x-1)^2 + 35(2x-1)^4]\}, \quad (8)$$

$$\phi^s_\rho(x) = \frac{3f^T_\rho}{2\sqrt{2N_c}}(1-2x)[1 + 0.76(10x^2 - 10x + 1)], \quad (9)$$

$$\phi^T_\rho(x) = \frac{3f^T_\rho}{\sqrt{2N_c}}x(1-x)[1 + 0.2C_2^{3/2}(2x-1)], \quad (10)$$

$$\phi^v_\rho(x) = \frac{f_\rho}{2\sqrt{2N_c}}\left\{\frac{3}{4}[1 + (2x-1)^2] + 0.24[3(2x-1)^2 - 1] + 0.12[3 - 30(2x-1)^2 + 35(2x-1)^4]\right\}, \quad (11)$$

$$\phi^a_\rho(x) = \frac{3f_\rho}{4\sqrt{2N_c}}(1-2x)[1 + 0.93(10x^2 - 10x + 1)], \quad (12)$$

with the Gegenbauer polynomials,

$$C_2^{1/2}(t) = \frac{1}{2}(3t^2 - 1), \quad C_4^{1/2}(t) = \frac{1}{8}(35t^4 - 30t^2 + 3),$$
$$C_2^{3/2}(t) = \frac{3}{2}(5t^2 - 1), \quad C_4^{3/2}(t) = \frac{15}{8}(21t^4 - 14t^2 + 1). \quad (13)$$

B. Perturbative calculations

For decay $B \to \rho\rho$, the related effective Hamiltonian is given by [21]

$$H_{\rm eff} = \frac{G_F}{\sqrt{2}}\bigg\{V_{ud}V_{ub}^*[C_1(\mu)O_1(\mu) + C_2(\mu)O_2(\mu)] - V_{tb}^*V_{td}\sum_{i=3}^{10}C_i(\mu)O_i(\mu)\bigg\}, \tag{14}$$

where $C_i(\mu)(i = 1, \cdots, 10)$ are Wilson coefficients at the renormalization scale μ and the four quark operators $O_i(i = 1, \cdots, 10)$ are

$$\begin{aligned} O_1 &= (\bar{b}_i u_j)_{V-A}(\bar{u}_j d_i)_{V-A}, \\ O_2 &= (\bar{b}_i u_i)_{V-A}(\bar{u}_j d_j)_{V-A}, \\ O_3 &= (\bar{b}_i d_i)_{V-A}\sum_q(\bar{q}_j q_j)_{V-A}, \\ O_4 &= (\bar{b}_i d_j)_{V-A}\sum_q(\bar{q}_j q_i)_{V-A}, \\ O_5 &= (\bar{b}_i d_i)_{V-A}\sum_q(\bar{q}_j q_j)_{V+A}, \\ O_6 &= (\bar{b}_i d_j)_{V-A}\sum_q(\bar{q}_j q_i)_{V+A}, \\ O_7 &= \frac{3}{2}(\bar{b}_i d_i)_{V-A}\sum_q e_q(\bar{q}_j q_j)_{V+A}, \\ O_8 &= \frac{3}{2}(\bar{b}_i d_j)_{V-A}\sum_q e_q(\bar{q}_j q_i)_{V+A}, \\ O_9 &= \frac{3}{2}(\bar{b}_i d_i)_{V-A}\sum_q e_q(\bar{q}_j q_j)_{V-A}, \\ O_{10} &= \frac{3}{2}(\bar{b}_i d_j)_{V-A}\sum_q e_q(\bar{q}_j q_i)_{V-A}. \end{aligned} \tag{15}$$

Here i and j are SU(3) color indices; the sum over q runs over the quark fields that are active at the scale $\mu = O(m_b)$, i.e., $q \in \{u, d, s, c, b\}$. Operators O_1, O_2 come from tree level interaction, while O_3, O_4, O_5, O_6 are QCD-penguin operators and O_7, O_8, O_9, O_{10} come from electroweak-penguins.

Similar to the $B \to \pi\pi$ decays [5], there are eight types of Feynman diagrams contributing to $B \to \rho^+\rho^-$ decay mode at leading order, which are shown in Fig. 1. They involve two types: the emission and annihilation topologies. Each type is classified into factorizable diagrams, where hard gluon connects the quarks in the same meson, and nonfactorizable diagrams, where hard gluon attaches the quarks in two different mesons. Through calculating these diagrams, we can get the amplitudes M_H, where $H = L, N, T$ standing for the longitudinal and two transverse polarizations. Because these diagrams are the same as those of $B \to \phi K^*$ [7] and $B \to K^*K^*$ [22], the formulas of $B \to \rho\rho$ are similar to those of $B \to \phi K^*$ or $B \to K^*K^*$.

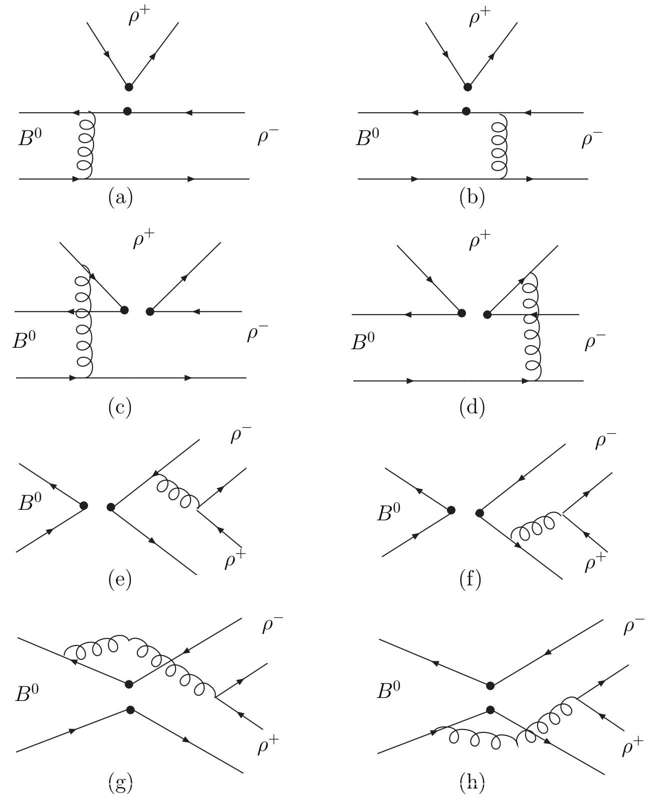

FIG. 1. The leading order Feynman diagrams for $B \to \rho\rho$.

We just need to replace some corresponding wave functions, Wilson coefficients, and corresponding parameters. So we do not present the detailed formulas in this paper.

III. NUMERICAL RESULTS FOR BRANCHING RATIOS AND POLARIZATIONS

In our calculation, some parameters such as meson mass, decay constants, the CKM matrix elements and the lifetime of B meson [23] are given in Table I.

Taking $B^0 \to \rho^+\rho^-$ as an example, we know that ($H = L, N, T$):

$$\begin{aligned} M_H &= V_{ub}^*V_{ud}T_H - V_{tb}^*V_{td}P_H \\ &= V_{ub}^*V_{ud}T_H(1 + z_H e^{i(-\alpha+\delta_H)}). \end{aligned} \tag{16}$$

TABLE I. Parameters we used in numerical calculation [23].

Mass	$m_{B^0} = 5.28$ GeV	$m_{B^+} = 5.28$ GeV
	$m_\rho = 0.77$ GeV	$m_\omega = 0.78$ GeV
Decay Constants	$f_B = 196$ MeV	$f_\rho = f_\omega = 200$ MeV
	$f_\rho^\perp = f_\omega^\perp = 160$ MeV	
CKM	$\lvert V_{ud}\rvert = 0.9745$	$\lvert V_{ub}\rvert = 0.042$
	$\lvert V_{td}\rvert = 0.0025$	$\lvert V_{tb}\rvert = 0.999$
Lifetime	$\tau_{B^0} = 1.54 \times 10^{-12}$ s	$\tau_{B^+} = 1.67 \times 10^{-12}$ s

TABLE II. Polarization amplitudes (10^{-3}GeV) of different diagrams in $B^0 \to \rho^+\rho^-$ decay.

Decay mode	(a) and (b)	(c) and (d)	(e) and (f)	(g) and (h)
$L(T)$	77	$-2.4 + 0.6i$	0	$-1.4 - 3.4i$
$L(P)$	-3.1	$0.14 + 0.03i$	$3.0 - 1.7i$	$0.39 + 0.57i$
$N(T)$	8.7	$1.3 - 0.05i$	0	$0.04 - 0.09i$
$N(P)$	-0.34	$-0.03 + 0.007i$	$1.6 + 0.8i$	$-0.002 + 0.009i$
$T(T)$	17	$2.7 - 0.004i$	$0.04 + 0.01i$	$0.002 - 0.008i$
$T(P)$	-1.8	$-0.07 + 0.02i$	$3.2 + 1.7i$	$0.004 + 0.004i$

with definition: CKM phase angle $\alpha = \arg[-\frac{V_{tb}V_{td}^*}{V_{ub}V_{ud}^*}]$ and $z_H = |\frac{V_{tb}V_{td}^*}{V_{ub}V_{ud}^*}||\frac{P_H}{T_H}|$. The strong phase δ_H and ratio z_H of tree (T) and penguin (P) are calculated in PQCD approach. In PQCD approach, the strong phases come from the nonfactorizable diagrams and annihilation type diagrams because quarks and gluons can be on mass shell. Numerical analysis also shows that the main contribution to the relative strong phase δ_H comes from the penguin annihilation diagrams. B meson annihilates into $q\bar{q}$ quark pair and then decays to $\rho\rho$ final states [1,24]. In the hadronic picture, the intermediate $q\bar{q}$ quark pair represents a number of resonance states, which implies final state interaction. These diagrams also make the contribution of penguin diagrams more important than previously expected.

In Table II, we show the numerical results of each diagram in $B^0 \to \rho^+\rho^-$ decay mode. From this table, we find that the most important contribution (about 95%) comes from the first two factorizable emission diagrams Fig. 1(a) and 1(b), especially for the longitudinal part. But the first two diagrams can not contribute to the relative strong phases. The main source of strong phases are from the annihilation diagrams, especially penguin diagrams of Fig. 1(e)–1(h). We can calculate that the strong phase for each polarization is $\delta_L = 13.6°$, $\delta_N = 42°$, and $\delta_T = 39°$.

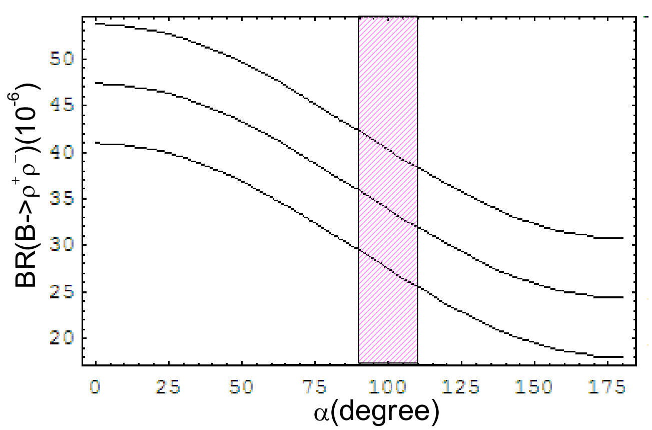

FIG. 2 (color online). Average branching ratio with theoretical uncertainty of $B^0 \to \rho^+\rho^-$ as a function of CKM angle α, where the shaded band shows the 1σ constraint for α.

In the same way, we can get the formula for the charged conjugate decay $\bar{B}^0 \to \rho^+\rho^-$:

$$\bar{M}_H = V_{ub}V_{ud}^* T_H(1 + z_H e^{i(\alpha+\delta_H)}). \quad (17)$$

Therefore, the averaged branching ratio for $B \to \rho^+\rho^-$ is

$$\mathcal{M}_H^2 \propto |V_{ub}^* V_{ud} T_H|^2 (1 + 2z_H \cos\alpha \cos\delta_H + z_H^2). \quad (18)$$

Here, we notice the branching ratio is a function of $\cos\alpha$. This $\cos\alpha$ behavior of the branching ratio is shown in Fig. 2. In principle, we can determine angle α through Eq. (18). However, the uncertainty of theory is so large (also shown in Fig. 2) as to make it unrealistic. First, the major uncertainty comes from higher order correction. In the calculation of $B \to K\pi$ [25], the results show that the next-to-leading order contribution can give about 15–20% correction to leading order. Second, the wave functions which describe the hadronic process of the meson are not known precisely, especially for the heavy B meson. Using the existing data of other channels such as $B \to \pi l \nu$ [26], $B \to D\pi$ [27], $B \to K\pi, \pi\pi$ [5], etc., we can fit the B meson wave function parameter $\omega_B = 0.4 \pm 0.1$. Another uncertainty comes from parameter c of threshold resummation[1], and it varies from 0.3 to 0.4. In leading order, considering the uncertainty taken by ω and c, we give the branching ratios and polarization fractions in Table III together with averaging experimental measurements [14–17].

There are still many other parameters existed such as decay constants, CKM elements, and we will not discuss the uncertainty here. The polarization fractions of these decay modes are not sensitive to the above parameters, because they mainly give an overall change of all polarization amplitudes, not to the individual noes. From our calculation, we find that these polarization fractions are sensitive to the distribution amplitudes of vector mesons. However, the distribution amplitudes we used are results from light-cone sum rules [20], which are difficult to change. Anyway, 20% uncertainty from the meson distribution amplitudes for the polarization fractions are possible. The range of CKM angle α has been well constrained

[1]The formula of threshold resummation [18] $S_t(x) = \frac{2^{1+2c}\Gamma(3/2+c)}{\sqrt{\pi}\Gamma(1+c)}[x(1-x)]^c$

TABLE III. Branching ratios and polarizations fractions of $B \to \rho(\omega)\rho(\omega)$ decays from theory and experiments [14–17]. In our results, the uncertainties come from ω_B and c respectively.

	BR(10^{-6})		f_L(%)			
Channel	Theory	Exp.	Theory	Exp.	$f_{\parallel}$(%)	$f_{\perp}$(%)
$B^0 \to \rho^+\rho^-$	$35 \pm 5 \pm 4$	30 ± 6	94	96^{+4}_{-7}	3	3
$B^+ \to \rho^+\rho^0$	$17 \pm 2 \pm 1$	$26.4^{+6.1}_{-6.4}$	94	99 ± 5	4	2
$B^+ \to \rho^+\omega$	$19 \pm 2 \pm 1$	$12.6^{+4.1}_{-3.8}$	97	88^{+12}_{-15}	1.5	1.5
$B^0 \to \rho^0\rho^0$	$0.9 \pm 0.1 \pm 0.1$	<1.1	60	...	22	18
$B^0 \to \rho^0\omega$	$1.9 \pm 0.2 \pm 0.2$	<3.3	87	...	6.5	6.5
$B^0 \to \omega\omega$	$1.2 \pm 0.2 \pm 0.2$	<19	82	...	9	9

as $\alpha = (98^{+6.1}_{-5.6})°$ [28], so that its small uncertainty affects very little on the branching ratios.

From above results and Table III, some discussions are in order:

(a) For simplicity, we set that the ρ^0, ω have same mass, decay constant and distribution amplitude. In quark model, the ρ^0 meson is $\frac{1}{\sqrt{2}}(u\bar{u} - d\bar{d})$, while ω is $\frac{1}{\sqrt{2}}(u\bar{u} + d\bar{d})$. The difference comes from the sign of $d\bar{d}$, which only appears in penguin operators, so their difference should be relatively small.

(b) For the tree dominant decays, most of the contribution to branching ratio comes from factorizable spectator diagram (a) and (b), which are the diagrams contribute to the $B \to \rho$ form factor. For example, in decay mode $B^0 \to \rho^+\rho^-$ the dominant Wilson coefficients are $C_2 + C_1/3$ (order of 1) at tree level, which is supported by numerical results. The decay $B^+ \to \rho^+\omega$ and $B^+ \to \rho^+\rho^0$ have the similar situation. Their branching ratios are all at the order 10^{-5}.

(c) For decay $B \to \rho^0\rho^0$, the Wilson coefficient is $C_1 + C_2/3$ in tree level, which is color suppressed. In this work, we only calculate the leading order diagrams, and did not calculate the higher order corrections. So, the Wilson coefficients we used are leading order results in order to keep consistency. In leading order, the sign of C_2 is positive while the sign of C_1 is negative, which can cancel each other mostly. Thus the branching ratio of $B \to \rho^0\rho^0$ is rather small. If considering next to leading order corrections, the sign of $C_1 + C_2/3$ may change to positive, so the branching ratio may become larger. This decay should be more sensitive to next leading order contribution. This is similar to the argument of $B^0 \to \pi^0\pi^0$ decay and $B^0 \to \rho^0\omega$, $\omega\omega$.

(d) Comparing our results with experiments (world average), we find both branching ratios and polarizations agree well with only one exception: $B^+ \to \rho^+\rho^0$. In fact, this is due to a large branching fraction measured by Belle [17],

$$\mathbf{B\,R}(B^+ \to \rho^+\rho^0) = (31.7 \pm 7.1^{+3.8}_{-6.7}) \times 10^{-6}, \quad (19)$$

which does not overlap with BaBar's data [14–16]

$$\mathbf{B\,R}(B^+ \to \rho^+\rho^0) = (22.5^{+5.7}_{-5.4} \pm 5.8) \times 10^{-6}. \quad (20)$$

We are waiting for the consistent results from two experimental groups. As for the color suppressed $B^0 \to \rho^0\rho^0$, $B^0 \to \rho^0\omega$ and $B^0 \to \omega\omega$, there are only upper limits now, and our results are still below the upper limits.

(e) In Ref. [12,29,30], these decay modes have been calculated in QCD factorization approach. For $B^0 \to \rho^+\rho^-$, the branching ratio they predicted is a bit larger than the experimental data, because the form factor they used is $V^{B\to\rho} = 0.338$. In PQCD approach [31], this form factor is about 0.318, so our results is smaller than theirs. Similar to above decay, our results in decay $B^+ \to \rho^+\rho^0$ is also smaller than the results in QCD factorization approach for the same reason. For decay modes $B^0 \to \rho^0\rho^0$, $B^0 \to \rho^0\omega$, and $B^0 \to \omega\omega$, our results are much larger than theirs because the annihilation diagrams play a very important role, and these parts cannot be calculated directly in QCD factorization approach.

(f) Both dominant by color enhanced tree contribution, we can see that the branching ratio of $B^0 \to \rho^+\rho^-$ is about two times of that of $B^+ \to \rho^+\rho^0$. But on the experimental side, the world average results of these decays do not have so much difference. Neither QCD factorization approach nor naive factorization can explain this small difference. The similar situation also appears in the decays $B \to \pi\pi$ [4,5]. Many people have tried to explain this puzzle [1,32]. But for the $B \to \rho\rho$ decays, it is still early, since the very small branching ratio of $B^0 \to \rho^0\rho^0$ by experiments contradicts with isospin symmetry. We have to wait for the experiments.

(g) From the Table III, we know that longitudinal polarization is dominant in decay $B^0 \to \rho^+\rho^-$, $B^+ \to \rho^+\rho^0$, and $B^+ \to \rho^+\omega$, which occupies more than 90% contribution, and is consistent with experimental data. These results are also consistent with the prediction in naive factorization [3], because the transverse parts are r_ρ^2 suppressed, where $r_\rho = m_\rho/m_B$. But for $B^0 \to \rho^0\rho^0$ decay, the tree emission diagrams are mostly cancelled in the Wilson coefficients. As we will see later in Table IV, the most important contributions for this decay are from the nonfactorizable tree diagrams in Fig. 1(c) and 1(d) and also the penguin diagrams. With an additional gluon, the transverse polarization in the nonfactorizable diagrams does not encounter helicity flip suppression. The transverse polarization is at the same order as longitudinal polarization, which can also be seen in the column (c) and (d) of Table III. This scenario is new from the mechanism of the

TABLE IV. Contribution from different parts in $B^0 \to \rho^+\rho^-$ and $B^0 \to \rho^0\rho^0$: full contribution in line (1), ignore annihilation contribution in line (2), without penguin operators in line (3), and without nonfactorization diagrams in line (4).

$B^0 \to \rho^+\rho^-$	BR(10^{-6})	$f_L(\%)$	$f_\parallel(\%)$	$f_\perp(\%)$
(1)	35	94	3	3
(2)	35	94	3	3
(3)	32	94	3	3
(4)	38	96	2	2
$B^0 \to \rho^0\rho^0$	BR(10^{-6})	$f_L(\%)$	$f_\parallel(\%)$	$f_\perp(\%)$
(1)	0.94	60	22	18
(2)	0.38	42	26	32
(3)	0.25	18	41	41
(4)	1.18	83	8.5	8.5

recently penguin dominant process $B \to \phi K^*$ [33], where the penguin annihilation guides the dominant transverse contribution. In fact, the $B^0 \to \omega\omega$ decay has a little larger longitudinal fraction is just due to the fact that there is no nonfactorizable emission tree contribution for this decay in isospin symmetry.

Now we turn to discuss the contribution of different diagrams, where $B^0 \to \rho^+\rho^-$ and $B^0 \to \rho^0\rho^0$ are taken as an example. In the Table IV, we consider full contribution in line (1), ignore annihilation contribution in line (2), without any penguin operator in line (3), and without the nonfactorization diagram in line (4). From this table, we can see that neither annihilation diagrams nor nonfactorizable diagrams can change the polarization fraction in decay $B^0 \to \rho^+\rho^-$. They only take about 4% contribution in this decay mode just because the emission diagram occupies a very large part of the contribution, which can also be seen from Table II. However, the penguin operators—especially in annihilation diagrams—play an important role in decay $B^0 \to \rho^0\rho^0$.

Of course, the final state interaction is very important in nonleptonic B decays. They can give $\mathcal{O}(10^{-6})$ corrections [24], but this cannot change the branching ratios much for decay modes $B^0 \to \rho^+\rho^-$ and $B^+ \to \rho^+\rho^0$ at order 10^{-5}. Thus, in these two decay modes, the final state interaction may not be important. However, in decay $B^0 \to \rho^0\rho^0$, the final state interaction may afford larger contribution than our calculation ($10^{-7} - 10^{-6}$), that is to say, our perturbative part may not be the dominant contribution. Although probably important, the hadronic effects are not intensively discussed in this paper, since they are beyond the topics of our PQCD approach. The contributions of these two sides can be determined by experiments.

IV. *CP* VIOLATION IN $B^0 \to \rho^+\rho^-$ AND $B^+ \to \rho^+\rho^0(\omega)$

Studying *CP* violation is an important task in B physics. In this section, we discuss the *CP* violation in $B^0 \to \rho^+\rho^-$ and $B^+ \to \rho^+\rho^0(\omega)$ decays. The uncertainty in $B^0 \to \rho^0\rho^0(\omega)$, $\omega\omega$ for branching ratios is so large that we will not discuss their *CP* violation here, though it is also very important. In decay modes $B^0 \to \rho^+\rho^-$ and $B^+ \to \rho^+\rho^0(\omega)$, the longitudinal part occupies nearly 95% contribution. So we will neglect the transverse parts in the following discussions.

Using Eqs. (16) and (17), the direct *CP* violating parameter is easily derived as a function of CKM angle α.

$$A_{CP}^{\rm dir} = \frac{|M^+|^2 - |M^-|^2}{|M^+|^2 + |M^-|^2} = \frac{-2z\sin\alpha\sin\delta_L}{1 + 2z_L\cos\alpha\cos\delta_L + z_L^2}, \tag{21}$$

which is shown in Fig. 3. The direct *CP* asymmetry is about $(-10 \pm 4)\%$ in decay $B^0 \to \rho^+\rho^-$. However, the direct *CP* in decay $B^+ \to \rho^+\rho^0$ is almost zero, because there is no QCD-penguin contribution while the electroweak penguin contribution is rather negligible. On the other hand, because of large penguin contribution, the direct *CP* in $B^+ \to \rho^+\omega$ is about $(-23 \pm 7)\%$, which is even larger than $B^0 \to \rho^+\rho^-$. The uncertainty in the above results come from $90° < \alpha < 110°$ and $0.3 < \omega_B < 0.4$ in the B meson wave function.

For the neutral B^0 decays, there is more complication from the $B^0 - \bar{B}^0$ mixing. The time dependence of *CP* asymmetry is

$$A_{CP} \simeq A_{CP}^{\rm dir}\cos(\Delta mt) + \sin(\Delta mt)a_{\epsilon+\epsilon'}, \tag{22}$$

where Δm is the mass difference between the two mass eigenstates of neutral B mesons. The $A_{CP}^{\rm dir}$ is already defined in Eq. (21), while the mixing-related *CP* violation parameter is defined as

$$a_{\epsilon+\epsilon'} = \frac{-2\,{\rm Im}(\lambda_{CP})}{1 + |\lambda_{CP}|^2}, \tag{23}$$

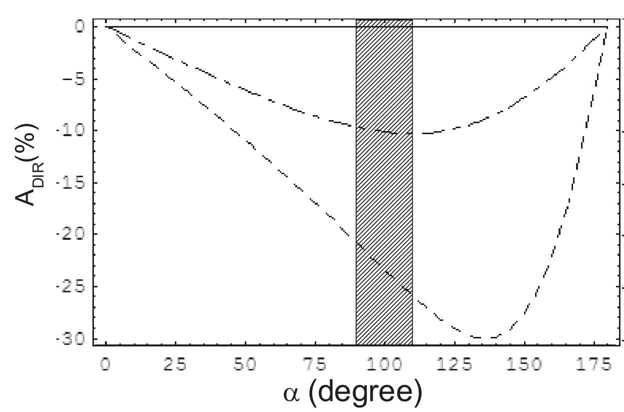

FIG. 3. Direct *CP* violation parameter $A_{CP}^{\rm dir}$ as a function of α with $\omega_B = 0.4$. The solid line is for $B^+ \to \rho^+\rho^0$, dashed-dotted line is for $B^0 \to \rho^+\rho^-$, and the dashed line is for $B^+ \to \rho^+\omega$. The shadow part is a band with $90° < \alpha < 110°$.

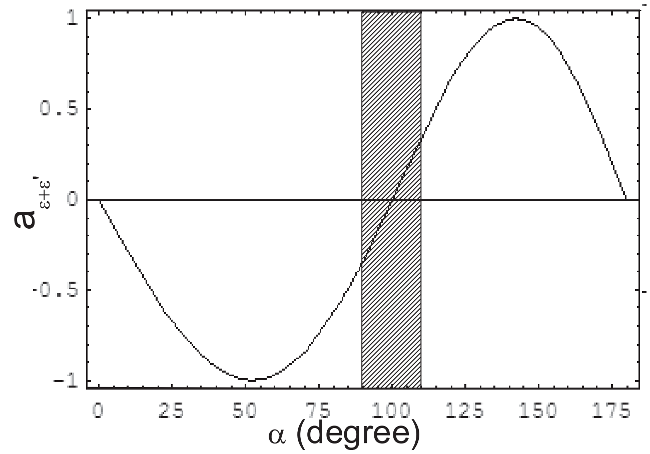

FIG. 4. Mixing induced CP violation parameters $a_{\epsilon+\epsilon'}$ of $B^0 \to \rho^+\rho^-$ as a function of CKM angle α with $\omega = 0.4$. The shadow part is a band with $90° < \alpha < 110°$.

where

$$\lambda_{CP} = \frac{V_{tb}^* V_{td}\langle f|H_{\rm eff}|\bar{B}|\rangle}{V_{tb}V_{td}^*\langle f|H_{\rm eff}|B\rangle}. \tag{24}$$

Using Eqs. (16) and (17), we derive

$$\lambda_{CP} \simeq e^{2i\alpha}\frac{1 + z_L e^{i(\delta_L - \alpha)}}{1 + z_L e^{i(\delta_L + \alpha)}}. \tag{25}$$

Thus, the parameter $a_{\epsilon+\epsilon'}$ is a function of α, if the penguin pollution is very small, $a_{\epsilon+\epsilon'}$ is about $-\sin 2\alpha$. From the function relation of Fig. 4, we can see that $a_{\epsilon+\epsilon'}$ is not exactly equal to $-\sin 2\alpha$, because of the penguin pollution.

If we integrate the time variable t of Eq. (22), we will get the total CP asymmetry as

$$A_{CP} = \frac{1}{1+x^2}A_{CP}^{\rm dir} + \frac{x}{1+x^2}a_{\epsilon+\epsilon'} \tag{26}$$

with $x = \Delta m/\Gamma \simeq 0.771$ for the $B^0 - \bar{B}^0$ mixing in SM [23]. Through calculating, we notice that the A_{CP} is $(-10 \pm 4)\%$ with uncertainty from $90° < \alpha < 110°$ and $0.3 < \omega_B < 0.4$.

V. SUMMARY

In this work, we calculate the branching ratios, polarizations and CP asymmetry of $B \to \rho(\omega)\rho(\omega)$ decays in perturbative QCD approach based on k_T factorization. After calculating all diagrams, including nonfactorizable diagrams and annihilation diagrams, we found that the branching ratios of $B^0 \to \rho^+\rho^-$ and $B^+ \to \rho^+\rho^0$ are at order of $\mathcal{O}(10^{-5})$, and the longitudinal contributions are more than 95%. These results agree with BaBar's data well. Moreover, we also predict the direct CP violation in $B^0 \to \rho^+\rho^-$ and $B^+ \to \rho^+\rho^0$, and mixing CP violation in $B^0 \to \rho^+\rho^-$, which may be important in extraction for the angle α. The longitudinal polarization for $B^0 \to \rho^0\rho^0$, $\rho^0\omega$, $\omega\omega$ are suppressed to 60–80% due to the large nonfactorizable tree contribution to these decays. These results can be tested in B factories in the future.

ACKNOWLEDGMENTS

This work is partly supported by the National Science Foundation of China. We thank C.-H. Chen for the useful discussion and G.-L. Song and D.-S. Du for reading the manuscript.

[1] A. J. Buras, R. Fleischer, S. Recksiegel, and F. Schwab, Phys. Rev. Lett. **92**, 101804 (2004); Nucl. Phys. **B697**, 133 (2004).
[2] M. Wirbel, B. Stech, and M. Bauer, Z. Phys. C **29**, 637 (1985); M. Bauer, B. Stech, and M. Wirbel, Z. Phys. C **34**, 103 (1987).
[3] A. Ali, G. Kramer, and C.-D. Lü, Phys. Rev. D **58**, 094009 (1998); Phys. Rev. D **59**, 014005 (1999); Y.-H. Chen, H.-Y. Cheng, B. Tseng, and K.-C. Yang, Phys. Rev. D **60**, 094014 (1999).
[4] M. Beneke, G. Buchalla, M. Neubert, and C. T. Sachrajda, Phys. Rev. Lett. **83**, 1914 (1999); Nucl. Phys. **B591**, 313 (2000); Nucl. Phys. **B675**, 333 (2003).
[5] H.-N. Li and H.-L. Yu, Phys. Rev. D **53**, 2480 (1996); Y.-Y. Keum, H.-N. Li, and A. I. Sanda, Phys. Rev. D **63**, 054008 (2001); C.-D. Lu, K. Ukai, and M.-Z. Yang, Phys. Rev. D **63**, 074009 (2001).
[6] C. W. Bauer, D. Pirjol, and I. W. Stewart, Phys. Rev. D **65**, 054022 (2002); Phys. Rev. D **63**, 114020 (2001).
[7] C.-H. Chen, Y.-Y. Keum, and H.-N. Li, Phys. Rev. D **66**, 054013 (2002).
[8] H.-W. Huang, *et al.*, hep-ph/0508080 [Phys. Rev. D (to be published)].
[9] A. L. Kagan, Phys. Lett. B **601**, 151 (2004).
[10] P. Colangelo, F. De. Fazio, and T. N. Pham, Phys. Lett. B **597**, 291 (2004).
[11] M. Ladisa, V. Laporta, G. Nardulli, and P. Santorelli, Phys. Rev. D **70**, 114025 (2004).
[12] Y.-D. Yang, R.-M. Wang, and G.-R. Lu, Phys. Rev. D **72**, 015009 (2005); S. Bar-shalom, A. Eilam, and Y.-D. Yang, Phys. Rev. D **67**, 014007 (2003).
[13] Y. Grossman, Int. J. Mod. Phys. A **19**, 907 (2004).
[14] B. Aubert *et al.* (BABAR Collaboration), Phys. Rev. Lett. **91**, 171802 (2003).
[15] B. Aubert *et al.* (BABAR Collaboration), Phys. Rev. D **69**, 031102 (2004).
[16] B. Aubert *et al.* (BABAR Collaboration), Phys. Rev. Lett. **95**, 041805 (2005).

[17] J. Zhang *et al.* (Belle Collaboration), Phys. Rev. Lett. **91**, 221801 (2003).
[18] H.-N Li, Phys. Rev. D **66**, 094010 (2002).
[19] C.-H Chang and H.-N Li, Phys. Rev. D **55**, 5577 (1997); T.-W Yeh and H.-N Li, Phys. Rev. D **56**, 1615 (1997).
[20] P. Ball and R. Zwicky, Phys. Rev. D **71**, 014029 (2005); P. Ball and V. M. Braun, Nucl. Phys. **B543**, 201 (1999).
[21] G. Buchalla, A. J. Buras, and M. E. Lautenbacher, Rev. Mod. Phys. **68**, 1125 (1996).
[22] J. Zhu, Y.-L. Shen, and C.-D. Lü, Phys. Rev. D **72**, 054015 (2005).
[23] S. Eidelman *et al.* (Particle Data Group), Phys. Lett. B **592**, 1 (2004).
[24] H.-Y. Cheng, Ch.-K. Chua, and A. Soni, Phys. Rev. D **71**, 014030 (2005).
[25] H.-N. Li, S. Mishima, and A. I. Sanda, Phys. Rev. D **72**, 114005 (2005).
[26] H.-N Li and H.-L. Yu, Phys. Rev. Lett. **74**, 4388 (1995).
[27] Y.-Y. Keum, T. Kurimoto, H.-N. Li, C.-D. Lü, and A. I. Sanda, Phys. Rev. D **69**, 094018 (2004).
[28] U. Nierste, plenary talk at "Lepton-Photon 2005," hep-ph/0511125.
[29] H.-Y. Cheng and K.-C. Yang, Phys. Lett. B **511**, 40 (2001).
[30] W.-J. Zou and Z.-J. Xiao, Phys. Rev. D **72**, 094026 (2005).
[31] C.-D. Lü and M.-Z. Yang, Eur. Phys. J. C **28**, 515 (2003).
[32] Y.-L. Wu and Y.-F. Zhou, Phys. Rev. D **72**, 034037 (2005); C. W. Bauer, D. Pirjol, I. Z. Rothstein, and I. W. Stewart, Phys. Rev. D **70**, 054015 (2004), and references therein.
[33] H.-N. Li, Phys. Lett. B **622**, 63 (2005); W.-S. Hou and M. Nagashima, hep-ph/0408007.